HHS Public Access

Author manuscript

Environ Sci Technol. Author manuscript; available in PMC 2018 December 19.

Published in final edited form as:

Environ Sci Technol. 2018 October 02; 52(19): 11319–11327. doi:10.1021/acs.est.8b03770.

Accelerated Oxidation of Organic Contaminants by Ferrate(VI): The Overlooked Role of Reducing Additives

Mingbao Feng[1], **Chetan Jinadatha**[2,3], **Thomas J. McDonald**[1], and **Virender K. Sharma**[1]

[1]Program for the Environment and Sustainability, Department of Environmental and Occupational Health, School of Public Health, Texas A&M University, College Station, Texas 77843, United States

[2]Central Texas Veterans Health Care System, 1901 Veterans Memorial Drive, Temple, Texas United States

[3]College of Medicine, Texas A and M Health Science Center, Department of Medicine, 8447 Riverside PKWY, Bryan, Texas United States

Abstract

This paper presents an accelerated ferrate(VI) ($Fe^{VI}O_4^{2-}$, Fe^{VI}) oxidation of contaminants in 30 s by adding one-electron and two-electron transfer reductants ($R_{(1)}$ and $R_{(2)}$). An addition of $R_{(2)}$ (e.g., NH_2OH, As^{III}, Se^{IV}, P^{III}, and NO_2^-, and $S_2O_3^{2-}$) results in Fe^{IV} initially, while Fe^{V} is generated with the addition of $R_{(1)}$ (e.g., SO_3^{2-}). $R_{(2)}$ additives, except $S_2O_3^{2-}$, show the enhanced oxidation of 20–40% of target contaminant, trimethoprim (TMP). Comparatively, enhanced oxidation of TMP was up to 100% with the addition of $R_{(1)}$ to Fe^{VI}. Interestingly, addition of $S_2O_3^{2-}$ (i.e., $R_{(2)}$) also achieves the enhanced oxidation to 100%. Removal efficiency of TMP depends on the molar ratio ($[R_{(1)}]$:$[Fe^{VI}]$ or $[R_{(2)}]$:$[Fe^{VI}]$). Most of the reductants have the highest removal at molar ratio of ~0.125. A Fe^{VI}–$S_2O_3^{2-}$ system also oxidizes rapidly a wide range of organic contaminants (pharmaceuticals, pesticides, artificial sweetener, and X-ray contrast media) in water and real water matrices. Fe^{V} and Fe^{IV} as the oxidative species in the Fe^{VI}–$S_2O_3^{2-}$-contaminant system are elucidated by determining removal of contaminants in oxygenated and deoxygenated water, applying probing agent, and identifying oxidized products of TMP and sulfadimethoxine (SDM) by Fe^{VI}–$S_2O_3^{2-}$ systems. Significantly, elimination of SO_2 from sulfonamide (i.e., SDM) is observed for the first time.

Graphical Abstract

Corresponding author: Virender K. Sharma, Phone: 979-436-9323, vsharma@sph.tamhsc.edu.

Associated Content

Notes

The authors declare no conflicts of interest.

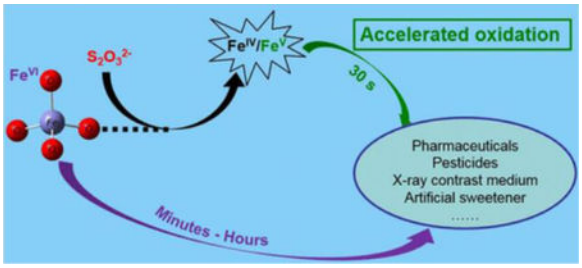

Introduction

Iron (Fe) is the second most abundant metal after aluminum in the earth's crust and is easily available. Iron plays many important roles in physiological processes, industrial synthesis, and remediation of pollutants in water.(1–7) In the decontamination field, iron-based technologies have been researched for many decades, including nanoscale zerovalent iron (nZVI), iron-based reactants/catalysts (e.g., Fe^{2+}, Fe^{3+}, Fe_3O_4, and Fe_2O_3) in advanced oxidation processes (Fe-AOPs), and high-valent iron-oxo units based systems (e.g., Fe^{IV}═O, Fe^{V}═O, and Fe^{VI}═O).(8–12) Among the high-valent iron remediation technologies, ferrate(VI) ($Fe^{VI}O_4^{2-}$, Fe^{VI}) has been receiving great attention due to its multiple roles as oxidant, disinfectant, and coagulant.(13–15) Examples include depollution of flue gases, pesticides, estrogens, and antibiotics, inactivation of bacteria, and viruses as well as coagulation of toxic metals and radionuclides.(15–17)

Fe^{VI} has shown high effectiveness in decontaminating organic pollutants from water. (12,15,18) However, oxidation of certain organics takes the time of minutes to hours to react with Fe^{VI}. This reactivity of Fe^{VI} decreases its oxidation capacity (i.e., electron equivalent per Fe^{VI}). Furthermore, due to simultaneous consumption of Fe^{VI} by unwanted reaction with water, a slow reaction with pollutants requires higher dosages of the oxidant, particularly at pH relevant to treatment conditions (pH 7.0 and 8.0).(15,19) These limitations restrict the applications of Fe^{VI} to efficiently oxidize a wide range of pollutants in water.

This paper presents a systematic innovative strategy to tune the chemistry of Fe^{VI} by selectively adding one-electron (S(IV)) and two-electron (or oxygen-atom transfer) reducing agents (hydroxylamine (NH_2OH), arsenite (AsO_3^{3-}), selenite (SeO_3^{2-}), phosphite (PO_3^{3-}), nitrite (NO_2^-), iodide (I^-), and thiosulfate ($S_2O_3^{2-}$)) (see Supporting Information (SI) Text S1)(20–25) that initially generate the short-lived Fe^{V} and Fe^{IV} species, respectively (i.e., $R_{(1)}$ (i.e., $Fe^{VI} \rightarrow Fe^{V}$),(26) and $R_{(2)}$ (i.e., $Fe^{VI} \rightarrow Fe^{IV}$)).(27) Fe^{V} and Fe^{IV} have 2–5 orders of reactivity higher than that of Fe^{VI} with reactivity order of $Fe^{V} > Fe^{IV} > Fe^{VI}$.(28–31) Our current results showed that the initially generated Fe^{V} had the highest enhancement (up to 100%), while oxygen-atom transfer reductants, except $S_2O_3^{2-}$, gave moderate enhancement (up to 40%) by producing Fe^{IV}. This feature of enhancement has not been reported in literature.

Recent studies carried out on enhancing the oxidation of contaminants in 15 s were restricted to few reductants that gave the contradictory results, and the description of observed findings was inconsistent.(32–34) In the earlier work on Fe^{VI}–S(IV) system,

enhancement was proposed solely due to activation of S(IV) by Fe^{VI} yielding $SO_3^{\bullet-}$, $SO4^{\bullet-}$, and $^{\bullet}OH$ without any role of intermediate Fe^{V}/Fe^{IV} species. Later work investigated the combined use of the reductants (S(IV), $S_2O_3^{2-}$, dithionite ($S_2O_4^{2-}$), pyrosulfite ($S_2O_5^{2-}$), and AsO_3^{3-}) with Fe^{VI} to oxidize N,N-diethyl-3-toluamide (DEET) in 10 s.(32) This study claimed that only sulfate radicals ($SO4^{\bullet-}$) caused the enhancement in the Fe^{VI}–S(IV) system.(32) Additionally, this study found no enhanced oxidation of DEET by adding $S_2O_3^{2-}$ and AsO_3^{3-} to Fe^{VI} at a high ratio (4:1) of [$S_2O_3^{2-}$/AsO_3^{3-}]:[Fe^{VI}].(32) Interestingly, our current study demonstrated the accelerated oxidation of contaminants by Fe^{VI} even using $S_2O_3^{2-}$ and AsO_3^{3-} when the ratio was much lower. Our previous work on Fe^{VI}–S(IV) system showed that multiple oxidizing species (Fe^{V}/Fe^{IV}, $SO_4^{\bullet-}$, and $^{\bullet}OH$) were responsible to cause enhancement of oxidation of antibiotics in water in 15 s.

Our work presented herein suggested that only Fe^{V}/Fe^{IV} species are involved in enhancing the oxidation of a wide range of contaminants in water at a lower ratio of [S(IV)/$S_2O_3^{2-}$]:[Fe^{VI}]. Importantly, we demonstrated the critical roles of molar ratios of $R_{(1)}/R_{(2)}$ to Fe^{VI} and kind of reductants (i.e., initial one-electron versus oxygen-atom transfer) to observe the magnitude of enhancement and involved oxidizing species in the combination of Fe^{VI} with the reductants. Moreover, SO_3^{2-} and $S_2O_3^{2-}$ are sulfur-based reductants but have different chemistry in reaction with Fe^{VI} (i.e., $R_{(1)}$ and $R_{(2)}$). We examined the Fe^{VI}–$S_2O_3^{2-}$ system in details for oxidizing a wide range of contaminants. We have applied density functional theory (DFT) calculations to demonstrate the two-electron transfer in the initial step of the Fe^{VI}–$S_2O_3^{2-}$ system. Also, $S_2O_3^{2-}$ was attractive to us because it is a commercially available salt with high stability. Comparatively, SO_3^{2-} is not stable in water(35) and is used in gaseous form (SO_2 (g)) at large facilities involving storage and handling issues. A system of Fe^{VI}–$S_2O_3^{2-}$ is an attractive alternate in enhancing oxidation of contaminants in large scale applications.

The objectives of current paper are to (i) demonstrate the enhanced reactivity of Fe^{VI} by adding $R_{(1)}$ and $R_{(2)}$ at trace levels with a focus on $S_2O_3^{2-}$ to decontaminate organics in water in 30 s. Sixteen organic contaminants of different categories and structures (artificial sweetener, pesticides, pharmaceuticals, and X-ray contrast medium, see SI Table S1) were selected. These compounds carry public health concerns and have shown low reactivity with Fe^{VI} alone,(12) (ii) identify the reactive oxidizing species causing accelerated oxidation of contaminants including recalcitrant compounds by Fe^{VI}-$R_{(1)}$ and Fe^{VI}-$R_{(2)}$ systems, (iii) learn the transformation products and reaction pathways of two representative pharmaceuticals (TMP and SDM) by Fe^{VI}-$R_{(1)}$ systems, and (iv) exhibit tuned reactivity of Fe^{VI} (i.e., Fe^{VI}–$S_2O_3^{2-}$ system) to rapidly remediate the organic contamination in real water matrices.

Materials and Methods

Chemicals and Reagents

Detailed information on all test organic contaminants, buffer chemicals and preparation of reaction solutions is provided in SI Text S2.

Oxidation of Organic Contaminants

All batch experiments were conducted in a series of 100 mL glass jars under constant stirring rate (400 rpm) with a magnetic stirrer. Elimination of each contaminant or their mixtures by Fe^{VI} with or without $S_2O_3^{2-}$ was initiated by mixing equal solution volumes of 10 mL, and the final pH values of reaction solutions were kept at 8.00 ± 0.05. The concentration of Fe^{VI} was maintained at 100.0 μM, and the ratios of $[S_2O_3^{2-}]$:$[Fe^{VI}]$ in the system varied from 0 to 5.0 for aqueous removal of TMP (5.0 μM). Similar removal experiments of TMP were performed by preadding seven other reducing agents (i.e., NH_2OH, AsO_3^{3-}, NO_2^-, SeO_3^{2-}, PO_3^-, I^-, and SO_3^{2-}) with different test concentrations, followed by Fe^{VI} oxidation. The optimized ratio of $[S_2O_3^{2-}]$:$[Fe^{VI}]$ at 1:8 (0.125) was used to oxidize all organic contaminants at environmentally relevant concentration (i.e., 1.0 μM) in either ultrapure water or real water samples (river and lake water). After 30 s of oxidation, a 20.0 μL NH_2OH solution (1 M, $[NH_2OH]$:$[Fe^{VI}]$ = 10.0) was added to quench the reactions. Samples were transferred into high performance liquid chromatography (HPLC) vials and subsequently analyzed using the HPLC method (see details in SI Text S3 and S4).

Analytical Procedures

Two inorganic reactive radicals (i.e., $^{\bullet}OH$ and/or $SO_4^{\bullet-}$), possibly produced in the oxidation system, were measured using the room-temperature electron paramagnetic resonance (EPR) technique.(34,36) Detailed information is provided in SI Text S4.

Results and Discussion

Fe^{VI}-$R_{(2)}$ Systems

Initially, accelerated removal of TMP by Fe^{VI} was examined at pH 8.0 by adding $R_{(2)}$ additives at various concentrations. Herein, tested $R_{(2)}$ act as two-electron transfer reducing species were evident through initial step of the reduction of Fe^{VI} by reductants. Initial steps of different reductants were supported by experimental finding using ^{18}O-labeled salt of Fe^{VI} (i.e., $K_2Fe^{18}O_4$) that demonstrated transfer of oxygen-atom from the oxidant to reductants (e.g., NO_2^- to NO_3^- and PO_3^{3-} to PO_4^{3-}).(24,37) The DFT calculations on the Fe^{VI}–AsO_3^{3-} system also provided preferable oxygen-atom transfer as first step of the reaction.(22,38) More details of the individual reductant as $R_{(2)}$ are given in SI Text S1.

Without $R_{(2)}$ additives, the removal of TMP by Fe^{VI} was ~16%, which rapidly increased following the introduction of $R_{(2)}$ into the Fe^{VI}-TMP mixed solution (Figure 1a). In solutions containing TMP and $R_{(2)}$ (i.e., no Fe^{VI}), no oxidation of TMP was observed (SI Figure S1). This suggested that the enhancement of TMP was due to the reactive species generated by the interactions between Fe^{VI} and $R_{(2)}$. The maximum removal of TMP oxidation for $R_{(2)}$ was up to ~25%, at a molar ratio of 0.1 ($[R_{(2)}]$:$[Fe^{VI}]$) (Figures 1a and b). At molar ratios greater than 0.1, enhanced oxidation of TMP decreased. At high levels of NH_2OH and AsO_3^{3-} (i.e., $[R_{(2)}]$:$[Fe^{VI}]$ = 10.0 and 5.0, respectively), oxidation of TMP ceased. Importantly, a molar ratio of 10.0 using hydroxylamine as a quenching reagent was sufficient to stop the oxidation of the contaminant by Fe^{VI}. Increasing the concentration of selenite resulted in an initial decrease to ~6%, followed by no effect due to further increase in the molar ratios of selenite to Fe^{VI} (Figure 1b). An increase in concentration of PO_3^{3-}

showed no decrease in removal of TMP (Figure 1b). This trend is similar to NO_2^-, in which the maximum removal of TMP was ~30% at a molar ratio of 1.0 (Figure 1c). In this additive, eliminating oxygen from the air by purging with nitrogen showed no difference in removal of TMP (Figure 1c).

The results shown in Figure 1 may be explained by the sequence of reactions taking place in the Fe^{VI}-$R_{(2)}$-TMP system (Reactions 1–5). In absence of $R_{(2)}$, TMP is oxidized only by Fe^{VI} (Reaction 1). However, when $R_{(2)}$ is added, Reaction 2 occurs, generating Fe^{IV} species (speculative as $HFe^{IV}O_3^-$), which can react with TMP (Reaction 3). Fe^{IV} species are much more reactive than parent Fe^{VI} and therefore, enhancement in removal of TMP was observed by adding $R_{(2)}$ to Fe^{VI}-TMP solutions (Figure 1). However, Fe^{IV} may also react with $R_{(2)}$ (Reaction 4). Self-decomposition reaction of Fe^{IV} may also happen (Reaction 5).(39)

$$HFe^{IV}O_4^- + TMP \rightarrow Fe^{3+} + TMP(oxidized) \quad (1)$$

$$HFe^{IV}O_4^- + R_{(2)} \rightarrow HFe^{IV}O_3^- + R_{(2)}(oxidized) \quad (2)$$

$$HFe^{IV}O_3^- + TMP \rightarrow Fe^{3+}/Fe^{2+} + TMP(oxidized) \quad (3)$$

$$HFe^{IV}O_3^- + R_{(2)} \rightarrow Fe^{3+}/Fe^{2+} + R_{(2)}(oxidized) \quad (4)$$

$$HFe^{IV}O_3^- + HFe^{IV}O_3^- + 3H_2O \rightarrow 2Fe(OH)_3 + 1/2O_2 + 2OH^- \quad (5)$$

Results of Figure 1 suggest that enhancement due to $R_{(2)}$ is related to the concentrations of generated Fe^{IV}, added $R_{(2)}$, and the competitive rate constants of Reactions 2–5. At low concentration of $R_{(2)}$, Fe^{IV} produced from Reaction 2 seems to be reacting with TMP (Reaction 3) to yield enhancements in removal (Figure 1). However, with increasing concentrations of $R_{(2)}$, Reaction 4 begins to dominate and causes the decreasing concentration of Fe^{IV}, that is, less Fe^{IV} species is available to oxidize TMP (i.e., TMP(oxidized products)), which results in the decreasing trend in the removal of TMP. Incomplete removal of TMP by the Fe^{VI}-$R_{(2)}$ system suggests that Reaction 5 may be significant to result in the disappearance of Fe^{IV} itself(39) rather than the oxidation of TMP.

The rate constants of Reactions 2–5, shown to describe results of Figure 1, are currently unknown in literature to describe fully enhancement in removal of TMP under Fe^{VI}-$R_{(2)}$ systems under studied conditions. Determination of these rate constants would require modified premix pulse radiolysis technique.(29,30,39) It seems that the rate constants of

Reactions 2 and 4 vary with the type of $R_{(2)}$, which gave different patterns of the oxidation of TMP with increasing molar ratios of $R_{(2)}$ to Fe^{VI}. Furthermore, Reactions 1–5 are a simplistic representation of involved reactions and complex chemistry, which may be existing in a particular Fe^{VI}-$R_{(2)}$ additive system.

Fe^{VI}-Iodide System

The addition of iodide resulted in ~41% removal at a molar ratio of 0.1 ($[I^-]$:$[Fe^{VI}]$) (Figure 2a). Further increase in this molar ratio decreased the removal of TMP, and complete inhibition of TMP was observed at the molar ratio of 1.0 (Figure 2a). A formation of I_3^- in the reaction of Fe^{VI} with I– has been observed, which produced through initial one-electron transfer step ($Fe^{VI} + I^- \rightarrow Fe^{V} + I^{\bullet}$) (SI Text S1).(20) The generated Fe^{V} may react with TMP to enhance the oxidation of TMP. However, a recent study proposed oxygen-atom transfer step that gave Fe^{IV} species in initial step ($Fe^{VI} + I^- \rightarrow Fe^{IV} + HOI/OI^-$) (SI Text S1).(40) The Fe^{IV} species may also increase the oxidation of TMP. Formation of different oxidized products has been observed in the reaction of O_3 with I^-.(41) Formed HOI has high reactivity with aromatic compounds, which suggests that TMP may also be oxidized by HOI in the Fe^{VI}–I^- system.(40) These reactive species would yield the enhanced oxidation of TMP observed in our study. It appears that at molar ratios greater than 0.1 ($[I^-]$:$[Fe^{VI}]$), the reactions of Fe^{V}/Fe^{IV} with I^- start competing with that of these intermediate iron species with TMP to cause decrease in enhanced effect of I^- to oxidize TMP.

Fe^{VI}-Sulfite System

Sulfite ion also showed the enhancement, with complete elimination of TMP at a molar ratio of 0.25 ($[SO_3^{2-}]$:$[Fe^{VI}]$) (Figure 2b). A detailed examination of the oxidation of SO_3^{2-} by Fe^{VI} showed that SO_3^{2-} acts as $R_{(1)}$ (see SI Text S1).(26) Enhanced oxidation of contaminants by Fe^{VI}–SO_3^{2-} system, studied only at a molar ratio of 4.0 ($[SO_3^{2-}]$:$[Fe^{VI}]$), was also reported in our previous study and other investigations.(32,34) Figure 2b shows that the increasing ratios had no decreasing effect on TMP removal until the molar ratio of 5.0. However, when the molar ratio was greater than 5.0, enhanced oxidation of TMP decreased and no enhancement could be obtained at the molar ratio of 20.0 (SI Figure S2). When nitrogen was purged in Fe^{VI}–SO_3^{2-}TMP solution, enhanced removal efficiency decreased, and maximum removal of TMP was ~83% in the molar ratio between 0.5 and 1.0 (Figure 2b). In the molar ratio range of 1.0–5.0, a linear decrease to 60% was observed in TMP removal (Figure 2b).

Reactions 6–10 may describe the results in Figure 2b. A SO_3^{2-} ion reduced Fe^{VI} to Fe^{V} with the formation of a $^{\bullet}SO_3-$ (Reaction 6, for example, $k_6 = (2.0 \pm 0.2) \times 10^1\ M^{-1}\ s^{-1}$, pH 11.4). This radical also reduced Fe^{VI} to give Fe^{V} (Reaction 7, for example, $k_7 = (1.9 \pm 0.3) \times 10^8\ M^{-1}\ s^{-1}$, pH 11.4).(26) Fe^{V} species react with TMP to enhance the oxidation of TMP (Reaction 8). Fe^{V} is 3–5 orders of magnitude higher in reactivity than Fe^{VI},(28) hence the observed enhancement in TMP oxidation (see Figure 2). Furthermore, Fe^{V} is much more reactive than Fe^{IV} species produced by $R_{(2)}$, and results in substantially more enhancement caused by $R_{(1)}$ compared to $R_{(2)}$ (Figure 2b versus Figure 1). However, Fe^{V} may react with SO_3^{2-} without the formation of Fe^{IV} species (Reaction 9, e.g., $k_9 = (3.9 \pm 0.4) \times 10^4\ M^{-1}\ s^{-1}$, pH 11.4).(26) The self-decomposition of Fe^{V} species to Fe^{III} may also occur (Reaction

10, k_{10} = (~7× 10^5 M^{-1} s^{-1}, pH 11.4).(42) Both Reactions 9 and 10 caused the elimination of the reactive Fe^V species, responsible for enhancing the removal of TMP.

$$HFe^{VI}O_4^- + SO_3^{2-} \rightarrow HFe^{V}O_4^{2-} + {}^{\bullet}SO_3^- \quad (6)$$

$$HFe^{VI}O_4^- + + {}^{\bullet}SO_3^- \rightarrow HFe^{V}O_4^{2-} + SO_3 \quad (7)$$

$$HFe^{V}O_4^{2-} + TMP \rightarrow Fe^{3+}/Fe^{2+} + TMP(oxidized) \quad (8)$$

$$HFe^{V}O_4^{2-} + SO_3^{2-} + 3H_2O \rightarrow Fe(OH)_3 + SO_4^{2-} \quad (9)$$

$$HFe^{V}O_4^{2-} + HFe^{V}O_4^{2-} + 4H_2O \rightarrow 2Fe(OH)_3 + O_2 + 4OH^- \quad (10)$$

Concentrations of Fe^V produced and TMP in Fe^{VI}–SO_3^{2-}-TMP solutions and the competitive rate constants of Reactions 6–10 at pH 8.0 would ultimately determine the magnitude of enhancement of the target contaminant and their variation with the ratio of SO_3^{2-} to Fe^{VI}. Additional oxidant species ($SO4^{\bullet-}$ and $^{\bullet}OH$) are formed ($SO_3 + 2OH^- \rightarrow SO_4^{2-} + H_2O$; ${}^{\bullet}SO_3^- + O_2 \rightarrow {}^{\bullet}SO_5^- \rightarrow\rightarrow {}^{\bullet}SO_4^-$; and ${}^{\bullet}SO_4^- + H_2O \rightarrow SO_4^{2-} + H^+ + {}^{\bullet}OH$),(34,43) in which no decrease in enhancement of TMP removal at [SO_3^{2-}]:[Fe^{VI}] = 0.1–5.0 is observed.(32,34) Formation of such radicals has been evidenced in previous investigations.(32,34) However, at ratios higher than 5.0, Reactions 9 and 10 are most likely to occur to cause the decrease in enhanced oxidation of TMP by Fe^{VI}–SO_3^{2-} system (SI Figure S2). Interestingly, when no oxygen existed in the solution mixture, enhanced oxidation of TMP still occurred. The values of rate constants for Reactions 7–9 at pH 8.0 are needed to fully understand the observed trend of enhancement in Figure 2b.

Fe^{VI}-Thiosulfate System

Enhancement of TMP removal was also seen when $S_2O_3^{2-}$ was used as a reductant, with complete removal of TMP observed at a ratio of 0.125 (Figure 2c). In the mixture of TMP-$S_2O_3^{2-}$ solutions, no removal of TMP was seen (SI Figure S1), therefore, the enhancement of TMP removal (Figure 2c) is due to this reducing additive in the Fe^{VI}-TMP mixed solution. Removal of oxygen (i.e., nitrogen purging) in Fe^{VI}–$S_2O_3^{2-}$-TMP solution had no significant difference from TMP removal in air saturated solutions (Figure 2c). At a molar ratio ([$S_2O_3^{2-}$]:[Fe^{VI}]) greater than 0.125, enhancement of TMP oxidation decreased. When this molar ratio reached 5.0, no oxidation of TMP occurred (or complete inhibition). The

magnitude of enhanced effect depends on the pH and the concentrations of contaminant (see SI Figure S3).

Based on the results observed in Figure 2c, $S_2O_3^{2-}$ as an additive was selected to investigate the acceleration and enhancement of 16 organic contaminants at pH 8.0. Except the unstable sulfite,(35) all other additives are pollutants and unsuitable for use as additives in treatment processes using Fe^{VI}. A molar ratio of $S_2O_3^{2-}$ to Fe^{VI} was selected at 0.125, which demonstrated complete removal of TMP. As shown in Figure 3, the presence of $S_2O_3^{2-}$ in the Fe^{VI}-contaminant system could increase the removal percentages of all contaminants in 30 s, as compared to Fe^{VI} only. Interestingly, complete removal of typical electron-rich moieties containing pharmaceuticals (CMZ, DCF, PPN, SDM, TMP, and ENR) was found, similar to oxidation of TMP (see Figure 2b). Notably, removals of other recalcitrant contaminants were also significant (20–40%). The results of Figure 3 suggest that a wide range of organic contaminants can be rapidly removed by the Fe^{VI}–$S_2O_3^{2-}$ system. Considering the coexistence of various pharmaceuticals in the water environment, elimination of six pharmaceuticals present in a mixture solution by the Fe^{VI}–$S_2O_3^{2-}$ system was also studied at pH 8.0. Again, complete removal of all tested contaminants was found after 30 s (SI Figure S4). These observations further suggest the applicability of $S_2O_3^{2-}$ in enhancing the oxidation of organic contaminants by Fe^{VI} in water.

Results of the Fe^{VI}–$S_2O_3^{2-}$ system at low molar ratios ($[S_2O_3^{2-}]$:$[Fe^{VI}]$ ≤0.125)) were similar to those obtained in the Fe^{VI}–SO_3^{2-} system. Our initial thought was that the Fe^{VI}–$S_2O_3^{2-}$ system may be generating directly Fe^{V} and $S2O3^{\bullet-}$ (Reaction 11) to result in enhanced oxidation of contaminants. However, experimental findings of the oxidation of $S_2O_3^{2-}$ by Fe^{VI} suggested oxygen atom transfer from Fe^{VI} to $S_2O_3^{2-}$ to produce Fe^{IV} and $S_2O_4^{2-}$ (Reaction 12 and see SI Text S1).

$$HFe^{VI}O_4^{-} + S_2O_3^{2-} \rightarrow HFe^{V}O_4^{2-} + S_2O_3^{\bullet-} \quad (11)$$

$$HFe^{VI}O_4^{-} + S_2O_3^{2-} \rightarrow HFe^{IV}O_3^{-}S_2O_4^{2-} \quad (12)$$

To further clarify whether $S_2O_3^{2-}$ behaves like $R_{(1)}$ additive (i.e., Reaction 11) or $R_{(2)}$ (i.e., Reaction 12), DFT calculations were performed to learn the favorable step of the reaction between Fe^{VI} and $S_2O_3^{2-}$ (SI Text S5). All the species involved were optimized and the changes of Gibbs free energy (ΔG) were individually calculated for Reactions 11 and 12. Compared to the positive value ($\Delta G = 34.66$ kJ/mol) of Reaction 11, Reaction 12 had a negative value ($\Delta G = -50.67$ kJ/mol), indicating the spontaneity of two-electron transfer reaction (SI Figure S5). Thus, the results of DFT calculations are also in good agreement with the prediction based on the relationship of the rate constant with the potential of redox pair, $S_2O_4^{2-}/S_2O_3^{2-}$.(27)

Notably, results of enhancement in the Fe^{VI}–$S_2O_3^{2-}$ system differed from those obtained in the Fe^{VI}-$R_{(2)}$ system (Figure 2b versus Figure 1). We therefore proposed that the reaction between Fe^{VI} and $S_2O_3^{2-}$ produced indirectly Fe^{V} species to cause initial enhancement seen in Figure 2c. The final oxidized product observed in the reaction between Fe^{VI} and $S_2O_3^{2-}$ is SO_3^{2-} (Reaction 13).(44,45)

$$4HFeO_4^- + 3S_2O_3^{2-} + 2OH^- + 3H_2O \rightarrow 4Fe(OH)_3 + 6SO_3^{2-} \quad (13)$$

The generated SO_3^{2-} produced Fe^{V} species (see Reaction 6) to result in initial enhancement of the oxidation of TMP in the Fe^{VI}–$S_2O_3^{2-}$ system. The second-order rate constants for the reactivity of Fe^{VI} with $S_2O_3^{2-}$ and S(IV) ($HSO_3^- + SO_3^{2-}$) are 6.01×10^3 M^{-1} s^{-1} and 1.9×10^4 M^{-1} s^{-1} at pH 8.0.(23,45,46) This suggests that produced SO_3^{2-} in Reaction 13 can react with Fe^{VI} to form Fe^{V} (see Reaction 6). Radicals, that is, $SO_4^{\bullet-}$ and $^{\bullet}OH$, can only be generated in the presence of oxygen.(34) Participation of $SO4^{\bullet-}$ and $^{\bullet}OH$ to cause this enhancement was ruled out by performing the experiments under nitrogen environment (i.e., no oxygen from air). In 30 s, Fe^{VI} would not produce significant oxygen from its self-decomposition.(47) Results showed no significant difference in enhancing the oxidation of TMP by Fe^{VI}–$S_2O_3^{2-}$ system (see Figure 2b). This suggests that oxygen has a minimal, if any, role in carrying out oxidation of TMP by Fe^{VI}–$S_2O_3^{2-}$ mixed solution in 30 s. Similar results were also observed in oxidizing other organic contaminants (i.e., no obvious difference with and without oxygen in oxidation of APT, ATL, CAF, DCF, and ENR, SI Figure S6), suggesting no possible role of $SO_4^{\bullet-}$ and $^{\bullet}OH$ in the enhanced oxidation of organic pollutants by Fe^{VI}–$S_2O_3^{2-}$ system.

The room-temperature electron paramagnetic resonance (EPR) measurements with 5,5-dimethyl-1-pyrroline-*N*-oxide (DMPO) as the spin trap reagent were conducted to probe the formation of $SO4^{\bullet-}$ and $^{\bullet}OH$.(34,36) Compared with the EPR spectrum of the Fe^{VI}-TMP-DMPO system, no new signal was observed after introducing $S_2O_3^{2-}$ at a low ratio (1:8) of [$S_2O_3^{2-}$]:[Fe^{VI}] (SI Figure S7). The observed EPR signals in the control group were assigned as $^{\bullet}OH$, generated at a low yield (<4%) by Fe^{VI} self-decay in water.(19) The unchanged EPR intensity indicated that no $SO_4^{\bullet-}$ was produced and also $^{\bullet}OH$ was not further formed in the Fe^{VI}–$S_2O_3^{2-}$ system, therefore not contributing to the significantly enhanced oxidation of organic contaminants. Similar results were observed following introduction of the lower ratio (1:8) of [SO_3^{2-}]:[Fe^{VI}] and [I^-]:[Fe^{VI}] (SI Figure S7). Furthermore, $SO_3^{\bullet-}$ can also be ruled out in the system: it is a precursor to the production of $SO_4^{\bullet-}$.(34,43)

The role of Fe^{IV}/Fe^{V} intermediates on Fe^{VI}–$S_2O_3^{2-}$-contaminant system was further explored using dimethyl sulfoxide (DMSO) as the probing reagent for the high-valent iron species. DMSO is selectively oxidized by Fe^{V}═O and Fe^{IV}═O species through oxygen atom transfer to produce the corresponding sulfone ($DMSO_2$).(11,48,49) Such reactions differ from the reaction pathways involved in radicals-based oxidation.(50) The oxidation of TMP was followed by adding 1 mM DMSO into Fe^{VI}–$S_2O_3^{2-}$-TMP system. Interestingly, oxidation of TMP was almost inhibited in the presence of DMSO (i.e., no difference in TMP removal by Fe^{VI} with and without $S_2O_3^{2-}$) (SI Figure S8). This suggests that the Fe^{IV}/Fe^{V}

species generated in Fe^{VI}–$S_2O_3^{2-}$-TMP solution were captured by DMSO and thus, unavailable to oxidize TMP. It should be pointed out that Fe^{VI} has a very slow reactivity with DMSO ($k \sim 1.0\ M^{-1}\ s^{-1}$ at pH 8.0)(51) and no significant reaction between Fe^{VI} and DMSO was expected in 30 s ($t_{1/2} \sim 690$ s). Therefore, the dominant reactive species for oxidation of organic pollutants in Fe^{VI}–$S_2O_3^{2-}$ system were Fe^{IV}/Fe^{V} species. Another study has reported different rate constant for the reaction of Fe^{VI} with DMSO (i.e., $16\ M^{-1}\ s^{-1}$, giving $t_{1/2}$ of Fe^{VI} consumption by 1 mM of DMSO = 43 s).(45) However, excessive Fe^{VI} (100.0 μM) used in our study would ensure the enhanced effect, which could still be seen at less magnitude because of less molar ratio of $S_2O_3^{2-}$ to Fe^{VI} than 0.125. As shown in SI Figure S8, the oxidation of TMP completely stopped by the presence of DMSO in the Fe^{VI}–$S_2O_3^{2-}$ system. In other words, both rate constants applied in previously reported studies suggest that the reaction of Fe^{VI} with DMSO had a minimal role, and inhibition of the degradation of TMP by the Fe^{VI}–$S_2O_3^{2-}$ system was due to elimination of Fe^{IV}/Fe^{V} species by DMSO; suggesting the generation of such highly reactive iron species to enhance the oxidation of contaminants by the Fe^{VI}–$S_2O_3^{2-}$ system. Additionally, the oxidized product of DMSO by the Fe^{VI}–$S_2O_3^{2-}$ system was identified as $DMSO_2$ (SI Figure S9).

Overall, enhanced oxidation of TMP by the Fe^{VI}–$S_2O_3^{2-}$ system was most likely by direct production of Fe^{IV} (Reaction 12) and indirect generation of Fe^{V} species (Reaction 6), which reacted with TMP (Reactions 3 and 8). With increasing concentration of $S_2O_3^{2-}$ (or $[S_2O_3^{2-}]$:$[Fe^{VI}]$). The intermediate reactive iron species, Fe^{IV} and Fe^{V}, may be removed by their reactions with $S_2O_3^{2-}$ (Reactions 14 and 15). Reaction 14 is presumably occurring through oxygen-atom transfer from Fe^{IV} to $S_2O_3^{2-}$ yielding Fe^{II}, similar to the one proposed earlier.(45) The rapid reaction of Fe^{V} with $S_2O_3^{2-}$ may also happen (e.g., $k_{15} = (2.1 \pm 0.1) \times 10^3\ M^{-1}\ s^{-1}$, pH 11.4). The Fe^{II}, produced in Reaction 14, may consume the main oxidant, Fe^{VI} (Reaction 16, that is, $k_{16} = \sim 10^5\ M^{-1}\ s^{-1}$, pH 12.1).(26) Reaction 16 would terminate the production of Fe^{V} and Fe^{IV}, the responsible species to cause enhanced oxidation of TMP by Fe^{VI}–$S_2O_3^{2-}$ system. Furthermore, the reductants $R_{(2)}$ would produce Fe^{II} as one of reduced species of Fe^{VI} (see Reaction 4 or 14) before converting to final Fe^{III} species (Reaction 16). It appears that excess $S_2O_3^{2-}$ (or $[S_2O_3^{2-}]$:$[Fe^{VI}] > 1.0$), not only eliminates the Fe^{IV}/Fe^{VI} species (Reactions 14 and 15), but also causes the consumption of Fe^{VI} (Reaction 15). It seems no Fe^{VI} was available to oxidize TMP at excess concentration of $S_2O_3^{2-}$ and no degradation of TMP was observed (see Figure 2c).

$$HFe^{IV}O_3^- + S_2O_3^{2-} \rightarrow Fe(OH)_2 + S_2O_4^{2-} \quad (14)$$

$$HFe^{V}O_4^{2-} + S_2O_3^{2-} + 2H_2O \rightarrow Fe(OH)_3 + S_2O_4^{2-} + 2OH^- \quad (15)$$

$$HFe^{VI}O_4^- + 3Fe(OH)_2 + 3H_2O \rightarrow 4Fe(OH)_3 + OH^- \quad (16)$$

Available rate constants for Reactions 15 and 16 are at high alkaline medium (i.e., pH 11.4 and 12.1), and these reactions would occur at much faster rates at pH 8.0. For example, the rate constant for the reaction of Fe^{VI} with Fe^{II} was estimated to be greater than 1.0×10^7 M^{-1} s^{-1} at pH 5.0.(19) The initial step of Reaction 16 produces Fe^{V} (i.e., $Fe^{VI} + Fe^{II} \rightarrow Fe^{V} + Fe^{III}$). The subsequent reaction of Fe^{V} with Fe^{II} would produce Fe^{IV} ($Fe^{V} + Fe^{II} \rightarrow Fe^{IV} + Fe^{III}$). Similarly, Fe^{IV} may also react with Fe^{II} to form Fe^{III} ($Fe^{V} + Fe^{II} \rightarrow 2Fe^{III}$), which may terminate reaction. The rate constant of Reaction 14 is not known. The pattern of the oxidation of TMP in Figures 1 and 2 as well as SI Figure S2 may be explained fully by knowing the rate constants of reactions involved in the oxidation of TMP by Fe^{VI}-reducing additive system. At a molar ratio of 0.125 ($[S_2O_3^{2-}]$:$[Fe^{VI}]$), contributions of different involved reactions in the system provide optimum levels of Fe^{IV}/Fe^{V} to cause maximum oxidation of TMP. Again, the values of rate constants of all possible reactions at different pH are needed to understand this optimum ratio of 0.125.

Oxidized Products (OPs) of TMP and SDM by Fe^{VI}–$S_2O_3^{2-}$ System

The OPs of TMP and SDM by Fe^{VI}–$S_2O_3^{2-}$ system were investigated at pH 8.0 and a molar ratio of 0.125 ($[S_2O_3^{2-}]$:$[Fe^{VI}]$), which had complete removal of contaminants (see Figure 3). Based on the molecular weights and previous study,(34) OPs of TMP were named as OP-338, OP-322, OP-308, OP-306, OP-304, OP-292, OP-212, and OP-196. MS/MS spectra and possible structures of the fragments of SDM and its OPs are presented in SI Figure S10. SDM has five fragments (*m/z* 218.02295, 156.07666, 108.04427, 92.04943, and 65.03873 (SI Figure S10a). These structures were proposed as the sequential losses of the aniline group from SDM (*m/z* 311.08060), the SO_2 group from *m/z* 218.02295, the amino and methoxyl groups from *m/z* 156.07666, the residual aniline group from SDM (*m/z* 311.08060) and the loss of $-NH_2C$ group from *m/z* 92.04943. OPs of SDM were classified as OP-356, OP-340, OP-327, OP-326, OP-324, OP-311, OP-295, and OP-276 (SI Figure S10b–-S10i). The molecular compositions of these OPs were suggested by the good mass error (<3 ppm) between the experimental and theoretical *m/z* values. Results are summarized in SI Tables S3 and S4.

Some of the OPs in the Fe^{VI}–$S_2O_3^{2-}$ system were not found in the oxidation of TMP and SDM by $SO_4^{\bullet-}$ and $^{\bullet}OH$ systems (SI Tables S3 and S4).(52–56) This again indicates the absence of $SO_4^{\bullet-}$ and $^{\bullet}OH$ species during the enhanced elimination of TMP and SDM by Fe^{VI}–$S_2O_3^{2-}$ system. OPs were also determined independently in the oxidation of TMP and SDM by Fe^{VI} alone, Fe^{VI}–I^-, and Fe^{VI}–SO_3^{2-}, which also yielded the same products as obtained by Fe^{VI}–$S_2O_3^{2-}$ system (SI Tables S3 and S4). This further suggests that the oxidizing species in the Fe^{VI}–I^-, Fe^{VI}–SO_3^{2-}, and Fe^{VI}–$S_2O_3^{2-}$ systems at this lower ratio were likely the same oxidants, that is, Fe^{IV}/Fe^{V} species.

The OPs and reaction pathways of TMP by the Fe^{VI}–$S_2O_3^{2-}$ system were the same as those reported earlier (SI Figure S11).(34) Based on the reaction mechanisms of Fe^{VI} oxidation of sulfonamides (e.g., sulfamethoxazole (SMX)) and the OPs of SDM produced by the other oxidation systems,(52,54,57) two initial transformation pathways of SDM by the Fe^{VI}–$S_2O_3^{2-}$ system are suggested (Figure 4). The salient feature of reaction pathways was the formation of OP-276 through SO_2 elimination and rearrangement of OP-340 (Pathway I).

The SO_2 elimination has been commonly suggested in the oxidation of sulfonamides by $SO_4^{\bullet-}$,(52,58) but was first observed in the oxidation of SDM by the Fe^{VI}-$R_{(1)}$ system. In pathway I, the amino group in the benzene ring of SDM was oxidized to generate OP-326, which was further oxidized to form OP-324 with NO group and OP-340 with NO_2 group at the same reaction moiety. Afterward, OP-356 was formed via hydroxylation of OP-340. A similar reaction pathway was reported in the oxidation of SMX by Fe^{VI} alone under basic and neutral pH conditions.(57) Transformation of OP-340 resulted in OP-276. Herein, the nitro group could have deactivated the benzene ring, but involvement of highly reactive Fe^{IV}/Fe^{V} species may achieve further reaction of OP-340 to give the formation of OP-356. Generally, Fe^{IV}/Fe^{V} species have shown activation of C–H bond of organic molecules.(59,60) Pathway II was initiated by deamination of SDM to produce OP-295, and then two sequential hydroxylations occurred to produce OP-311 and OP-327, respectively (Figure 4). Deamination of SDM may be similar to the finding observed in oxidation of amino acids by ferrate species.(61,62) Formation of hydroxylated products (i.e., OP-311 and OP-327) may be occurring through involvement of Fe^{IV}/Fe^{V} species. A similar hydroxylation of the benzene ring of the parent molecule has also been observed in the oxidation of SMX and flumequine by Fe^{VI} alone.(57,63) Furthermore, we have independently studied the oxidation of benzene by Fe^{VI} and Fe^{VI}–$S_2O_3^{2-}$ systems at pH 8.0 after 30 s. The formation of phenol, generated by hydroxylation of benzene and confirmed by the HPLC spectra of the phenol standard, was observed in both systems (SI Figure S12). Molar yields of phenols were low (without thiosulfate: $[\text{phenol}]_{\text{formed}}/[\text{Fe(VI)}]_{\text{consumed}} = 0.41\ \mu M/6.5\ \mu M \approx 0.06$; with thiosulfate: $[\text{phenol}]_{\text{formed}}/[\text{Fe(VI)}]_{\text{consumed}} = 0.83\ \mu M/43.0\ \mu M \approx 0.02$). High-valent iron species produced in the system of Fe^{VI}–$S_2O_3^{2-}$ would react with phenol to give additional products. This may explain lower molar ratio of formed phenol to consumed Fe^{VI}. Reactivity of Fe^{V} with phenol is three-orders of magnitude higher than the reactivity of Fe^{VI} with phenol.(47) An independent study on the reaction of Fe(V) with phenol has shown several products are formed.(47) A detailed investigation of the oxidized products in the system of Fe^{VI}-thiosulfate-benzene would clarify this possibility. Nevertheless, hydroxylation of benzene by high-valent species is very likely as suggested by our results. Basically, the generation of Fe^{IV}/Fe^{V} species caused hydroxylation of benzene. This is supported by an independent DFT study on the reactivity of Fe^{IV} species with benzene.(64) Calculations showed the feasibility of the formation of phenol from the hydroxylation of benzene by Fe^{IV} species.

Environmental Implications

The results clearly demonstrate that the establishment of a Fe^{VI}-reducing agent system is a highly effective tool to generate high-valent iron-oxo intermediates for rapid water depollution. This was further tested in applying the Fe^{VI}–$S_2O_3^{2-}$ system in different water matrices. Investigated six pharmaceuticals were CMZ, DCF, ENR, PPN, SDM, and TMP at 1.0 μM. An optimum molar ratio of 0.125 ($[S_2O_3^{2-}]$:$[Fe^{VI}]$) at pH 8.0 was applied to investigate oxidation of these pharmaceuticals in both river water and lake water. The reactions were quenched in 30 s, and results are depicted in SI Figure S13. Interestingly, $S_2O_3^{2-}$ addition to Fe^{VI} could also enhance the removal percentages of target pharmaceuticals present in river water and lake water. In river water, four of the six pharmaceuticals could be removed completely (SI Figure S13a). Removal of CMZ and ENR

was ~80%. In lake water, removal of pharmaceuticals was less than that in river water (SI Figure S13b). Eliminations of DCF, PPN, SDM, and TMP were ~80%, whereas removal of CMZ and ENR was ~50%. It is likely that water constituents in natural waters such as anions, cations, and dissolved organic matters are influencing the removal of the target contaminants by the oxidizing species present in the Fe^{VI}–$S_2O_3^{2-}$ mixed solution. These results demonstrated that Fe^{VI}–$S_2O_3^{2-}$ system can be adopted for efficient and rapid remediation of natural waters polluted with organic micropollutants. However, dosages (or amount) of Fe^{VI} for eliminating organic contaminants would vary with the characteristics of treated water. In the application of Fe^{VI}–$S_2O_3^{2-}$ system, the formed products are nontoxic $Fe(OH)_3$ and SO_4^{2-}. Furthermore, generated $Fe(OH)_3$ has remarkable efficiency of removing metals and phosphate.(65–67)

Significantly, some of the reducing agents (e.g., $S_2O_3^{2-}$, NH_2OH, and NO_2^-) have been applied to quench the reaction between Fe^{VI} and contaminants without realizing that the added quencher may greatly influence the oxidative processes. Significantly, quenching the reaction depends on the molar ratio of quencher to Fe^{VI}, which varies with the type of quencher. For example, this study suggested ten times more molar concentration of NH_2OH than that of Fe^{VI} would be needed to inhibit the reaction of Fe^{VI} with the target contaminant. However, if $S_2O_3^{2-}$ is used to quench the reaction, only five-time the concentration of $S_2O_3^{2-}$ compared to Fe^{VI} would be sufficient. The results presented herein will guide researchers in future studies on the oxidation of contaminants by Fe^{VI}.

Supplementary Material

Refer to Web version on PubMed Central for supplementary material.

Acknowledgements

We thank anonymous reviewers for their comments, which improved the paper greatly. We also thank Dr. J. Clayton Baum for his guidance on density functional theory calculations.

References

1. Bauer I; Knölker H Iron catalysis in organic synthesis. Chem. Rev 2015, 115 (9), 3170–3387. [PubMed: 25751710]
2. Usman M; Byrne JM; Chaudhary A; Orsetti S; Hanna K; Ruby C; Kappler A; Haderlein SB Magnetite and green rust: Synthesis, properties, and environmental applications of mixed-valent iron minerals. Chem. Rev 2018, 118 (7), 3251–3304. [PubMed: 29465223]
3. Fukuzumi S; Lee Y; Nam W Mechanisms of two-electron versus four-electron reduction of dioxygen catalyzed by earth-abundant metal complexes. ChemCatChem 2018, 10 (1), 9–28.
4. Cussó O; Cianfanelli M; Ribas X; Klein Gebbink RJM; Costas M Iron catalyzed highly enantioselective epoxidation of cyclic aliphatic enones with aqueous H_2O_2. J. Am. Chem. Soc 2016, 138 (8), 2732–2738. [PubMed: 26799660]
5. Ma L; Lam WWY; Lo P; Lau K; Lau T Ca^{2+}-induced oxygen generation by FeO_4^{2-} at pH 9–10. Angew. Chem., Int. Ed 2016, 55 (9), 3012–3016.
6. Chen J; Draksharapu A; Harvey E; Rasheed W; Que L; Browne WR Direct photochemical activation of non-heme Fe(IV)O complexes. Chem. Commun 2017, 53 (91), 12357–12360.
7. Pandey B; Jaccob M; Rajaraman G Mechanistic insights into intramolecular ortho-amination/hydroxylation by nonheme Fe^{IV}═NTs/Fe^{IV}═O species: the *s* vs. the p channels. Chem. Commun 2017, 53 (22), 3193–3196.

8. Li J; Zhang X; Sun Y; Liang L; Pan B; Zhang W; Guan X Advances in sulfidation of zerovalent iron for water decontamination. Environ. Sci. Technol 2017, 51 (23), 13533–13544. [PubMed: 29135239]
9. Sun M; Chu C; Geng F; Lu X; Qu J; Crittenden J; Elimelech M; Kim J Reinventing Fenton chemistry: Iron oxychloride nanosheet for pH-insensitive H_2O_2 activation. Environ. Sci. Technol. Lett 2018, 5 (3), 186–191.
10. Mills MR; Weitz AC; Hendrich MP; Ryabov AD; Collins TJ NaClO-generated iron(IV) oxo ad iron(V)oxo TAML in pure water. J. Am. Chem. Soc 2016, 138, 13866–13869.
11. Li H; Shan C; Pan B Fe(III)-doped g-C_3N_4 mediated peroxymonosulfate activation for selective degradation of phenolic compounds via high-valent iron-oxo species. Environ. Sci. Technol 2018, 52 (4), 2197–2205. [PubMed: 29373017]
12. Sharma VK; Chen L; Zboril R Review on high valent Fe^{VI} (ferrate): A sustainable green oxidant in organic chemistry and transformation of pharmaceuticals. ACS Sustainable Chem. Eng 2016, 4, 18–34.
13. Liu Y; Wang L; Huang Z; Wang X; Zhao X; Ren Y; Sun S; Xue M; Qi J; Ma J Oxidation of odor compound indole in aqueous solution with ferrate(VI): Kinetics, pathway, and the variation of assimilable organic carbon. Chem. Eng. J 2018, 331, 31–38.
14. Karlesa A; De Vera GAD; Dodd MC; Park J; Espino MPB; Lee Y Ferrate(VI) oxidation of ß-lactam antibiotics: Reaction kinetics, antibacterial activity changes, and transformation products. Environ. Sci. Technol 2014, 48 (17), 10380–10389. [PubMed: 25073066]
15. Sharma VK; Zboril R; Varma RS Ferrates: Greener oxidants with multimodal action in water treatment technologies. Acc. Chem. Res 2015, 48, 182–191. [PubMed: 25668700]
16. Zhao Y; Han Y; Ma T; Guo T Simultaneous desulfurization and denitrification from flue gas by ferrate(VI). Environ. Sci. Technol 2011, 45 (9), 4060–4065. [PubMed: 21466216]
17. Machalová Šišková K; Jancula D; Drahoš B; Machala L; Babica P; Alonso PG; Trávnícek Z;Tucek J; Maršálek B; Sharma VK; Zboril R High-valent iron (Fe^{VI}, Fe^{V}, and Fe^{IV}) species in water: Characterization and oxidative transformation of estrogenic hormones. Phys. Chem. Chem. Phys 2016, 18 (28), 18802–18810. [PubMed: 27344983]
18. Feng M; Wang Z; Dionysiou DD; Sharma VK Metal-mediated oxidation of fluoroquinolone antibiotics in water: A review on kinetics, transformation products, and toxicity assessment. J. Hazard. Mater 2018, 344, 1136–1154. [PubMed: 28919428]
19. Lee Y; Kissner R; Von Gunten U Reaction of ferrate(VI) with ABTS and self-decay of ferrate(VI): Kinetics and mechanisms. Environ. Sci. Technol 2014, 48 (9), 5154–5162. [PubMed: 24697210]
20. Kralchevska RP; Sharma VK; Machala L; Zboril R Ferrates (Fe^{VI}, Fe^{V}, and Fe^{IV}) oxidation of iodide: Formation of triiodide. Chemosphere 2016, 144, 1156–1161. [PubMed: 26461440]
21. Johnson MD; Hornstein BJ The kinetics and mechanism of the ferrate(VI) oxidation of hydroxylamines. Inorg. Chem 2003, 42, 6923–6928. [PubMed: 14552644]
22. Lee Y; Um I; Yoon J Arsenic(III) oxidation by iron(VI) (Ferrate) and subsequent removal of arsenic(V) by iron(III) coagulation. Environ. Sci. Technol 2003, 37, 5750–5756. [PubMed: 14717190]
23. Johnson MD; Bernard J Kinetics and mechanism of the ferrate oxidation of sulfite and selenite in aqueous media. Inorg. Chem 1992, 31, 5140–5142.
24. Hightower SM; Lorenz BB; Bernard JG; Johnson MD Oxidation of phosphorus centers by ferrate(VI): Spectral observation of an intermediate. Inorg. Chem 2012, 51 (12), 6626–6632. [PubMed: 22663068]
25. Carr JD Kinetics and product identification of oxidation by ferrate(VI) of water and aqueous nitrogen containing solutes. ACS Symp. Ser 2008, 985 (Ferrates), 189–196.
26. Sharma VK; Cabelli DE Reduction of oxyiron(V) by sulfite and thiosulfate. J. Phys. Chem. A 2009, 113, 8901–8906. [PubMed: 19603757]
27. Sharma VK Oxidation of inorganic compounds by Ferrate (VI) and Ferrate(V): One-electron and two-electron transfer steps. Environ. Sci. Technol 2010, 44 (13), 5148–5152. [PubMed: 20527775]
28. Sharma VK Ferrate(V) oxidation of pollutants: A premix pulse radiolysis. Radiat. Phys. Chem 2002, 65, 349–355.

29. Bielski BHJ; Sharma VK; Czapski G Reactivity of ferrate(V) with carboxylic acids: a pre-mix pulse radiolysis study. Radiat. Phys. Chem 1994, 44 (5), 479–484.
30. Cabelli DE; Sharma VK Aqueous ferrate(V) and ferrate(IV) in alkaline medium: Generation and reactivity. ACS Symp. Ser 2008, 985 (Ferrates), 158–166.
31. Terryn RJ; Huerta-Aguilar CA; Baum JC; Sharma VK Fe^{VI}, Fe^{V}, and Fe^{IV} oxidation of cyanide: Elucidating the mechanism using density functional theory calculations. Chem. Eng. J 2017, 330, 1272–1278.
32. Sun S; Pang S; Jiang J; Ma J; Huang Z; Zhang J; Liu Y; Xu C; Liu Q; Yuan Y The combination of ferrate(VI) and sulfite as a novel advanced oxidation process for enhanced degradation of organic contaminants. Chem. Eng. J 2018, 333, 11–19.
33. Zhang J; Zhu L; Shi Z; Gao Y Rapid removal of organic pollutants by activation sulfite with ferrate. Chemosphere 2017, 186, 576–579. [PubMed: 28810226]
34. Feng MB; Sharma VK Enhanced oxidation of antibiotics by ferrate(VI)-sulfur(IV) system: Elucidating multi-oxidant mechanism. Chem. Eng. J 2018, 341, 137–145.
35. Zhang J; Millero FJ The rate of sulfite oxidation in seawater. Geochim. Cosmochim. Acta 1991, 55 (3), 677–685.
36. Feng M; Qu R; Zhang X; Sun P; Sui Y; Wang L; Wang Z Degradation of flumequine in aqueous solution by persulfate activated with common methods and polyhydroquinone-coated magnetite/multi-walled carbon nanotubes catalysts. Water Res 2015, 85, 1–10. [PubMed: 26281959]
37. McLaughlin CW Oxidation of nitrite ions and chlorine-containing compounds by potassium ferrate(VI) Ph.D. Dissertation, The Graduate College in the University of Nebraska, Lincoln, NE, 1984.
38. Sung M; Liu GH A DFT study on oxygen atom transfer reaction between ferrate ion and arsenite ion. ACS Symp. Ser 2016, 1238, 439–472.
39. Menton JD; Bielski BHJ Studies of the kinetics, spectral and chemical properties of Fe(IV) pyrophosphate by pulse radiolysis. Radiat. Phys. Chem 1990, 36, 725–733.
40. Shin J; von Gunten U; Reckhow DA; Allard S; Lee Y Reactions of ferrate(VI) with iodide and hypoiodous acid: Kinetics, pathways, and implications for the fate of iodine during water treatment. Environ. Sci. Technol 2018, 52 (13), 7458–7467. [PubMed: 29856214]
41. Pillar EA; Guzman MI; Rodriguez JM Conversion of iodide to hypoiodous acid and iodine in aqueous microdroplets exposed to ozone. Environ. Sci. Technol 2013, 47 (19), 10971–10979. [PubMed: 23987087]
42. Rush JD; Bielski BHJ Kinetics of ferrate(V) decay in aqueous solution. A pulse-radiolysis study. Inorg. Chem 1989, 28, 3947–3951.
43. Neta P; Huie RE Free-radical chemistry of sulfite. Environ. Health Perspect 1985, 64, 209–217. [PubMed: 3830699]
44. Read JF; John J; MacPherson J; Schaubel C; Theriault A The kinetics and mechanism of the oxidation of inorganic oxysulfur compounds by potassium ferrate. Part I. Sulfite, thiosulfate and dithionite ions. Inorg. Chim. Acta 2001, 315 (1), 96–106.
45. Johnson MD; Read JF Kinetics and mechanism of the ferrate oxidation of thiosulfate and other sulfur-containing species. Inorg. Chem 1996, 35, 6795–6799. [PubMed: 11666845]
46. Sharma VK Oxidation of inorganic contaminants by ferrates (Fe(VI), Fe(V), and Fe(IV)) - Kinetics and mechanisms - A review. J. Environ. Manage 2011, 92, 1051–1073. [PubMed: 21193263]
47. Rush JD; Cyr JE; Zhao Z; Bielski BH The oxidation of phenol by ferrate(VI) and ferrate(V). A pulse radiolysis and stopped-flow study. Free Radical Res 1995, 22 (4), 349–360. [PubMed: 7633565]
48. Pestovsky O; Bakac A Aqueous ferryl(IV) ion: Kinetics of oxygen atom transfer to substrates and oxo exchange with solvent water. Inorg. Chem 2006, 45, 814–820. [PubMed: 16411719]
49. Bataineh H; Pestovsky O; Bakac A pH-induced mechanistic changeover from hydroxyl radicals to iron(IV) in the Fenton reaction. Chem. Sci 2012, 3 (5), 1594–1599.
50. Pang S; Jiang J; Ma J Oxidation of sulfoxides and arsenic(III) in corrosion of nanoscale zero valent iron by oxygen: Evidence against ferryl ions (Fe(IV)) as active intermediates in Fenton reaction. Environ. Sci. Technol 2011, 45 (1), 307–312. [PubMed: 21133375]

51. Bartzatt RL Kinetic of oxidation of various organic substrates by potassium ferrate Ph.D. Dissertation, University of Nebraska, Lincoln, NE, 1982.
52. Ji Y; Shi Y; Wang L; Lu J; Ferronato C; Chovelon J Sulfate radical-based oxidation of antibiotics sulfamethazine, sulfapyridine, sulfadiazine, sulfadimethoxine, and sulfachloropyridazine: Formation of SO_2 extrusion products and effects of natural organic matter. Sci. Total Environ 2017, 593–594, 704–712.
53. Ji Y; Xie W; Fan Y; Shi Y; Kong D; Lu J Degradation of trimethoprim by thermo-activated persulfate oxidation: Reaction kinetics and transformation mechanisms. Chem. Eng. J 2016, 286, 16–24.
54. Guerard JJ; Chin Y; Mash H; Hadad CM Photochemical fate of sulfadimethoxine in aquaculture waters. Environ. Sci. Technol 2009, 43 (22), 8587–8592. [PubMed: 20028056]
55. Zhang R; Yang Y; Huang CH; Li N; Liu H; Zhao L; Sun P UV/H_2O_2 and UV/PDS treatment of trimethoprim and sulfamethoxazole in synthetic human urine: Transformation products and toxicity. Environ. Sci. Technol 2016, 50 (5), 2573–2583. [PubMed: 26840504]
56. Yang H; Zhuang S; Hu Q; Hu L; Yang L; Au C; Yi B Competitive reactions of hydroxyl and sulfate radicals with sulfonamides in Fe^{2+}/S_2O82- system: Reaction kinetics, degradation mechanism and acute toxicity. Chem. Eng. J 2018, 339, 32–41.
57. Kim C; Panditi VR; Gardinali PR; Varma RS; Kim H; Sharma VK Ferrate promoted oxidative cleavage of sulfonamides: Kinetics and product formation under acidic conditions. Chem. Eng. J 2015, 279, 307–316.
58. Feng Y; Wu D; Deng Y; Zhang T; Shih K Sulfate radical-mediated degradation of sulfadiazine by $CuFeO_2$ rhombohedral crystal-catalyzed peroxymonosulfate: Synergistic effects and mechanisms. Environ. Sci. Technol 2016, 50 (6), 3119–3127. [PubMed: 26906407]
59. Cho K; Hirao H; Shaik S; Nam W To rebound or dissociate? This is the mechanistic question in C-H hydroxylation by heme and nonheme metal-oxo complexes. Chem. Soc. Rev 2016, 45 (5), 1197–1210. [PubMed: 26690848]
60. Serrano-Plana J; Oloo WN; Acosta-Rueda L; Meier KK; Verdejo B; García-España E; Basallote MG; Münck E; Que L; Company A; Costas M Trapping a highly reactive nonheme iron intermediate that oxygenates strong C-H bonds with stereoretention. J. Am. Chem. Soc 2015, 137 (50), 15833–15842. [PubMed: 26599834]
61. Rush JD; Bielski BHJ The oxidation of amino acid by ferrate(V). A pre-mix pulse radiolysis study. Free Radical Res 1995, 22, 571–579. [PubMed: 7633578]
62. Sharma VK; Bielski BHJ Reactivity of ferrate(VI) and ferrate(V) with amino acids. Inorg. Chem 1991, 30, 4306–4311.
63. Feng M; Wang X; Chen J; Qu R; Sui Y; Cizmas L; Wang Z; Sharma VK Degradation of fluoroquinolone antibiotics by ferrate(VI): Effects of water constituents and oxidized products. Water Res 2016, 103, 48–57. [PubMed: 27429354]
64. Li J; Zhang X; Huang XR Mechanism of benzene hydroxylation by high-valent bare $Fe^{IV}{=}O^{2+}$: Explicit electronic structure analysis. Phys. Chem. Chem. Phys 2012, 14 (1), 246–256. [PubMed: 22068928]
65. Lee Y; Zimmermann SG; Kieu AT; von Gunten U Ferrate (Fe(VI)) application for municipal wastewater treatment: A novel process for simultaneous micropollutant oxidation and phosphate removal. Environ. Sci. Technol 2009, 43, 3831–3838. [PubMed: 19544895]
66. Kralchevska RP; Prucek R; Kolarík J; Tucek J; Machala L; Filip J; Sharma VK; Zboril R Remarkable efficiency of phosphate removal: Ferrate(VI)-induced in situ sorption on core-shell nanoparticles. Water Res 2016, 103, 83–91. [PubMed: 27438903]
67. Prucek R; Tucek J; Kolarík J; Hušková I; Filip J; Varma RS; Sharma VK; Zboril R Ferrate(VI)-prompted removal of metals in aqueous media: Mechanistic delineation of enhanced efficiency via metal entrenchment in magnetic oxides. Environ. Sci. Technol 2015, 49 (4), 2319–2327. [PubMed: 25607569]

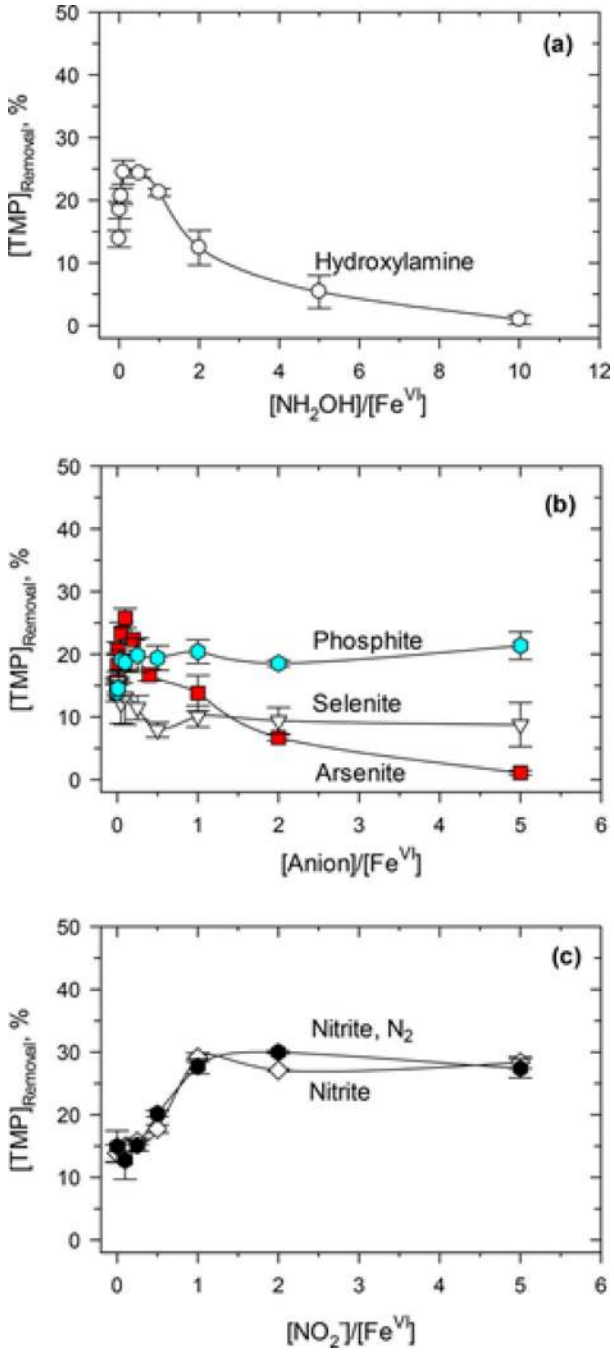

Figure 1.

Oxidation of TMP by Fe^{VI} and two-electron reducing additives ($R_{(2)}$, a, hydroxylamine; b, phosphite, selenite, and arsenite) system in air saturated solutions, and (c) nitrite under air saturated and anoxic conditions. (Experimental conditions: $[TMP]_0$ = 5.0 μM, $[Fe^{VI}]_0$ = 100.0 μM, pH 8.00 ± 0.05, reaction time = 30 s).

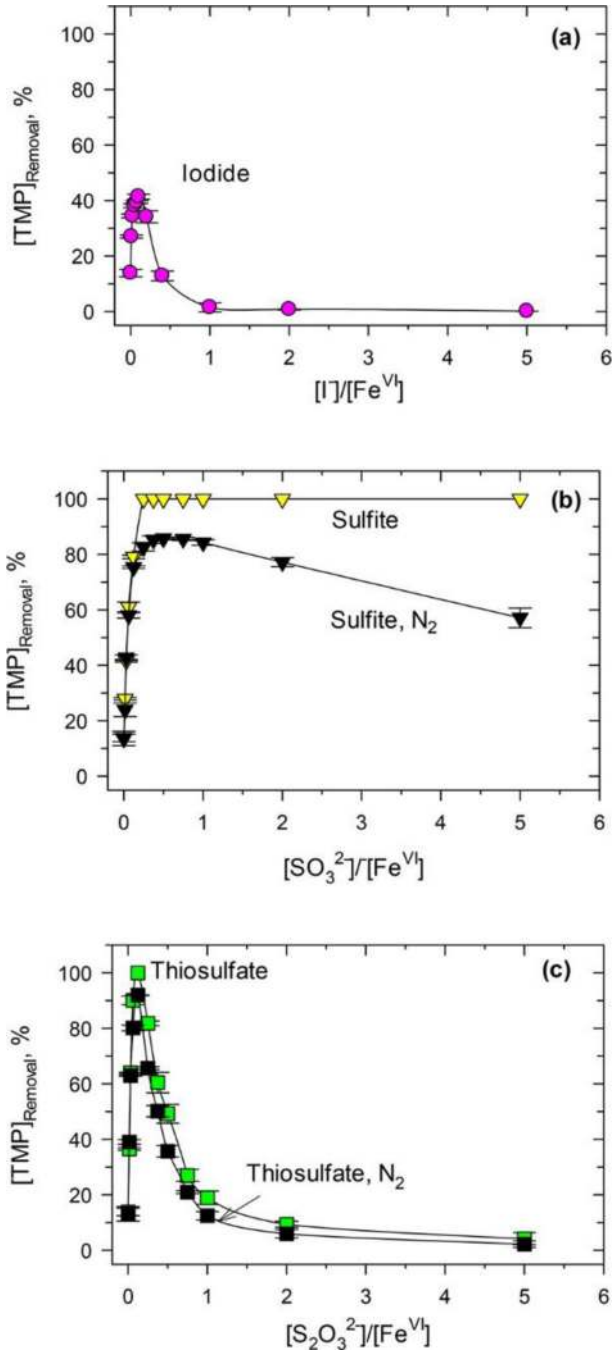

Figure 2.

Oxidation of TMP by Fe^{VI}-iodide (a), Fe^{VI}-sulfite (b), and Fe^{VI}-thiosulfate (c) systems in air saturated solutions. (Experimental conditions: $[TMP]_0$ = 5.0 μM, $[Fe^{VI}]_0$ = 100.0 μM, pH 8.00 ± 0.05, reaction time = 30 s).

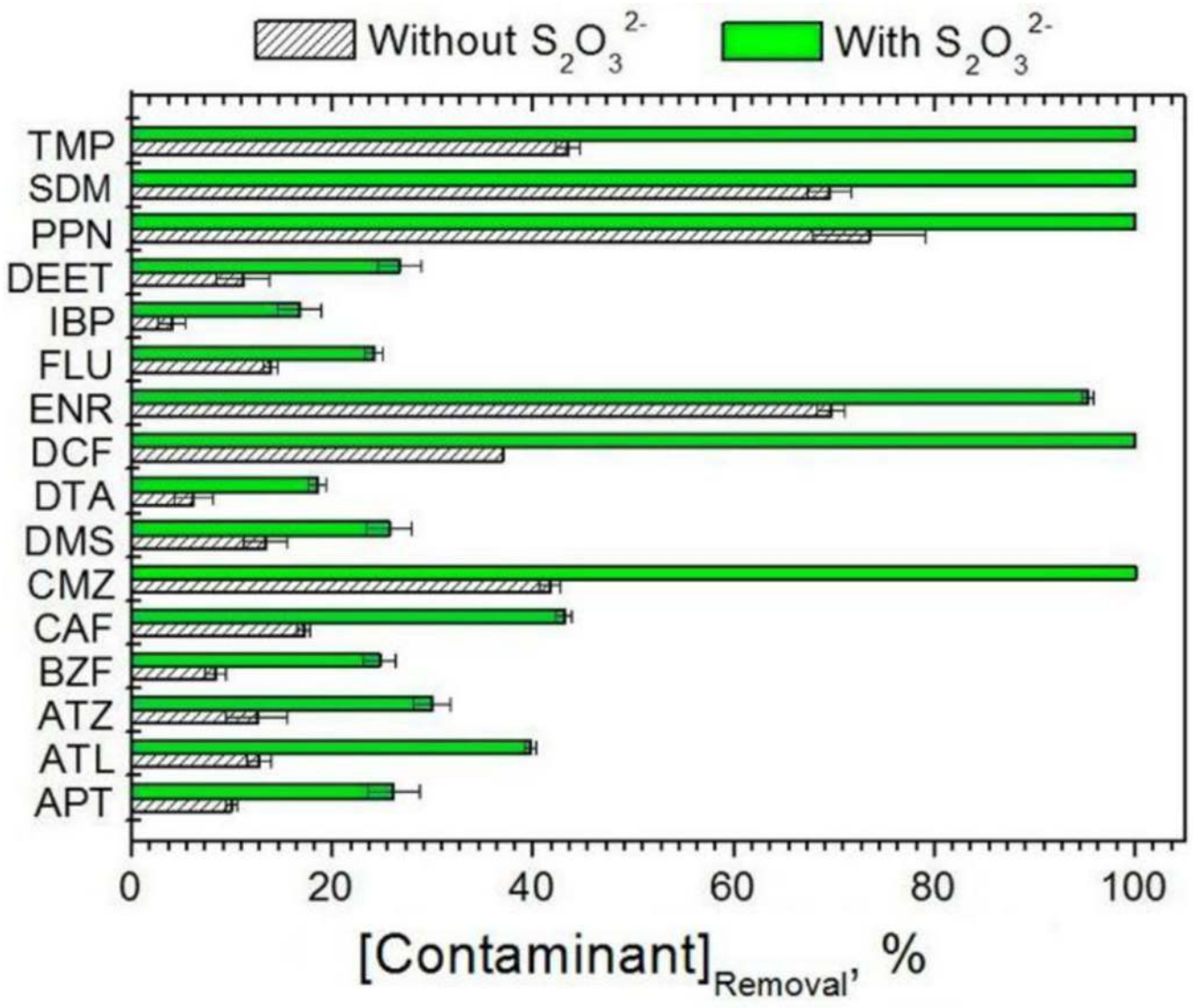

Figure 3.

Oxidation of organic contaminants by Fe^{VI} with and without $S_2O_3^{2-}$ in air saturated solution. (Experimental conditions: $[Contaminant]_0$ = 1.0 μM, $[Fe^{VI}]_0$ = 100.0 μM, $[S_2O_3^{2-}]_0$ = 12.5 μM, pH 8.00 ± 0.05, reaction time = 30 s). (APT-aspartame, ATL-atenolol, ATZ-atrazine, BZF-bezafibrate, CAF-caffeine, CMZ-carbamazepine, DMS-dexamethasone, DTA-diatrizoic acid, DCF-diclofenac, ENR-enrofloxacin, FLU-flumequine, IBP-ibuprofen, DEET-*N,N*-diethyl-3-toluamide, PPN-propranolol, SDM-sulfadimethoxine, TMP-trimethoprim).

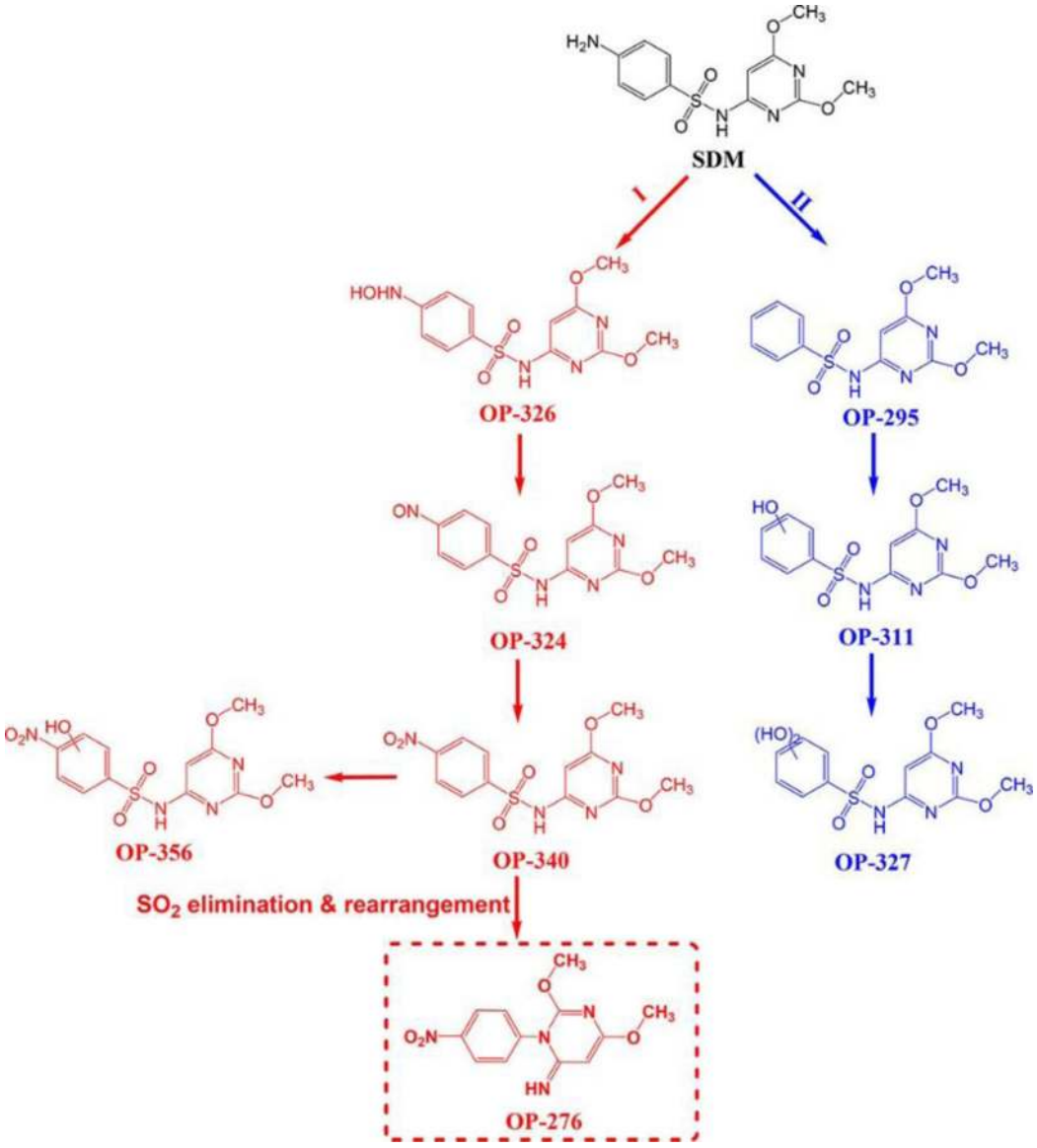

Figure 4.

Proposed reaction pathways of sulfadimethoxine (SDM) by Fe^{VI}–$S_2O_3^{2-}$ system at pH 8.00 in air saturated solution.